Shape coexistence and signature splitting in ^{77}Br

G. N. Sylvan and J. E. Purcell
Department of Physics and Astronomy, Georgia State University, Atlanta, Georgia 30303

J. Döring, J. W. Holcomb, G. D. Johns, T. D. Johnson,* M. A. Riley, P. C. Womble,† V. A. Wood, and S. L. Tabor
Department of Physics, Florida State University, Tallahassee, Florida 32306
(Received 25 May 1993)

High angular momentum states in ^{77}Br were populated via the ^{65}Cu(^{18}O,α2n)^{77}Br reaction at 65 MeV using the Florida State University (FSU) FN Tandem-LINAC accelerator. The Pitt-FSU array with 9 Compton-suppressed high purity Ge detectors was used to measure prompt γ-γ coincidences. Analysis of the coincidences led to an extension of the positive- and negative-parity bands to spins of $(\frac{41}{2}^+)$ and $(\frac{43}{2}^-)$. Directional correlation of oriented nuclei ratios have been deduced where possible, and spin assignments made accordingly. A cranked-shell-model analysis shows that in the positive-parity band the $\nu g_{9/2}$ alignment occurs at the same frequency as in the neighboring isotopes, ^{75,79}Br, but with a larger interaction strength. In the negative-parity bands the lower $\pi g_{9/2}$ crossing also occurs at about the same frequency as in ^{75}Br, but with a smaller interaction. The higher frequency $\nu g_{9/2}$ crossing is delayed in ^{77}Br. Hartree-Fock-Bogolyubov cranking calculations predict considerable γ softness in ^{77}Br, and particle-rotor model calculations support the interpretation of γ softness or variations in triaxiality within the bands.

PACS number(s): 21.60.Cs, 21.60.Ev, 23.20.Lv, 27.50.+e

I. INTRODUCTION

Nuclei in the f-p-g shell exhibit a wide variety of shapes, and the nuclear shapes are often strongly influenced by individual nucleons. In some cases, such as ^{81}Sr [1], prolate and oblate shapes coexist at almost the same energy, and in many cases the nuclear shape is soft toward changes in the triaxiality parameter γ. Within a family of odd-Z isotopes or odd-N isotones, which should have similar single-particle configurations, γ may vary considerably, as has been observed in the $N = 41$ isotones [2].

The light isotopes of Br ($Z = 35$) [3–9] and Rb ($Z = 37$) [10–14] are strongly deformed, but sometimes [14] γ soft. Another common feature of these odd-A Br and Rb isotopes is very large signature splitting in the $g_{9/2}$ yrast bands, leading to level inversion in most cases. Because of the inversion, the band of unfavored signature $\alpha = -\frac{1}{2}$ ($\frac{7}{2}^+$, $\frac{11}{2}^+$, etc.) is often difficult to locate and identify. It is not known in ^{73}Br [4] although the band of favored signature has been studied up to spin $\frac{45}{2}^+$. Four states in the unfavored band have been identified in ^{75}Br [5], where the favored positive-parity band is also known up to spin $\frac{45}{2}^+$. Before the present work, the level scheme of ^{77}Br had been explored only half as high in spin as its lighter neighbors, and differences existed in the literature concerning spin assignments in candidates for the band of unfavored signature. The present investigation of the high-spin structure of ^{77}Br was undertaken to resolve questions about the unfavored band, whose position provides information about the degree of triaxiality, and to compare its band structure with that of its better-known neighbors.

Two previous studies [7, 8] of excited states in ^{77}Br using the ^{75}As(α,2n)^{77}Br reaction established three positive-parity and two negative-parity decay sequences. The earlier study [7] established the positive-parity yrast band to the $(\frac{21}{2}^+)$ level at 2548 keV. The negative-parity band based on the $\frac{5}{2}^-$ state at 161.8 keV was established to $\frac{17}{2}^-$ at 2337.5 keV and another negative-parity band which decays directly to the $\frac{3}{2}^-$ ground state was established to $\frac{11}{2}^-$ at 1273.2 keV. An additional positive-parity band of undetermined spin was found.

The later study [8] extended the yrast band to $(\frac{25}{2}^+)$ at 3774 keV. The negative-parity bands were extended to $(\frac{25}{2}^-)$ at 4248 keV and $(\frac{23}{2}^-)$ at 3729 keV. The additional positive-parity band from the earlier work [7] was extended, with spin assignments, to $(\frac{21}{2}^+)$ at 3037 keV. An additional high-K, high-lying band was established based on a $(\frac{17}{2}^-)$ state at 2931.6 keV, and a positive-parity band based on a $\frac{7}{2}^+$ state at 417.5 keV was found. Aligned angular momentum calculations suggested that this band could be the unfavored signature partner to the yrast band.

Mean lifetimes have been measured [15] for the lower-spin states in ^{77}Br using the recoil-distance method. Enhanced $B(E2)$ strengths were found for transitions within the bands which were consistent with particle-

*Present address: II Physikalishes Institut, Bunsenstrasse 7-9, D37073 Göttinger, Federal Republic of Germany.
†Present address: Martin Marietta Energy Systems, Oak Ridge, TN 37831.

rotor model calculations based on a nuclear shape with a quadrupole deformation of $\beta_2 = 0.3$.

In the present work, a γ-γ coincidence measurement has confirmed these bands and extended them up to spins of $(\frac{41}{2}^+)$ and $(\frac{43}{2}^-)$. Measurements of the directional correlation of oriented nuclei ratios have provided firm spin assignments up to spins of $\frac{37}{2}^+$ and $\frac{33}{2}^-$. A cranked-shell-model analysis of moments of inertia, band crossings, and signature splittings has revealed systematic similarities and differences with the neighboring odd-A Br isotopes. The Hartree-Fock-Bogolyubov cranking calculations predict a deformation similar to what was observed experimentally, but with considerable γ softness. A comparison of the level scheme with particle-rotor model calculations supports the interpretation of γ softness and variable triaxiality in the bands.

II. EXPERIMENTAL METHODS

The ^{65}Cu(^{18}O,$\alpha 2n$) reaction was used to populate high-spin states in ^{77}Br. The Florida State University (FSU) Tandem-LINAC facility was used to accelerate ^{18}O to 65 MeV. The target was an 0.6 mg/cm^2 rolled Cu foil enriched to 99% in ^{65}Cu. Typical beam current on target was 40 nA electrical.

Prompt γ-γ coincidences were detected with the Pitt-FSU combined detector array [16]. Nine Compton-suppressed Ge detectors were used during this experiment. Three of the detectors were placed at 90° relative to the beam line, two were at 35°, and four at 145°. Each of the detectors was placed approximately 18 cm from the target. The energy calibrations of the detectors were determined from known lines in ^{76}Br, ^{78}Kr, ^{79}Kr, and ^{80}Kr in the on-line spectra. This provided an automatic compensation for Doppler shifting since all the evaporation residues travel at nearly the same velocity.

Approximately 1.8×10^8 coincidence events were recorded, about 15% of which involved ^{77}Br. After converting each detector channel number into energy, the coincidence events were histogrammed into a triangular array [17] with a dispersion of 0.8 keV/channel. This was the primary data set used for construction of the level scheme. A second square array was constructed by sorting those events in which a 90° and either a 35° or 145° detector fired. Since the 35° and 145° detectors are symmetric with respect to 90°, this array, with 90° data on one axis and 35° or a 145° data on the other, provided the information needed to determine the directional correlation of oriented (DCO) nuclei ratios to help assign spins.

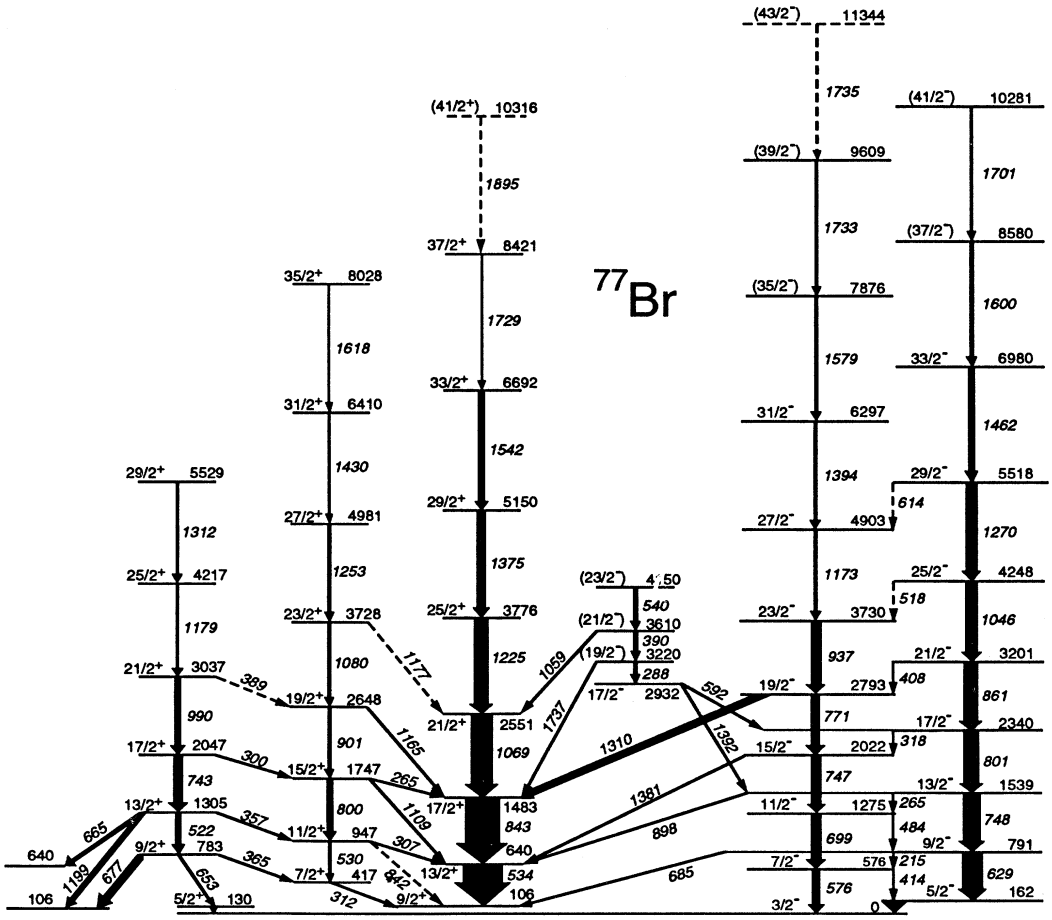

FIG. 1. The level scheme of ^{77}Br deduced from the present work.

III. THE LEVEL SCHEME

The present level scheme, shown in Fig. 1, was deduced from coincidence spectra generated by gating on the triangular and square two-dimensional arrays. Placement in the level scheme and relative intensities were determined from the triangular array. Multipolarities of the transitions were assigned based on the DCO ratios where possible, and on systematics where not. In the latter cases, the spins are shown in parentheses in Fig. 1. The $R_{\rm DCO}$ values were computed from coincidence spectra in the square array, comparing intensities according to

$$R_{\rm DCO} = \frac{I_\gamma \text{ (at } 35°/145° \text{ gated by } \gamma_G \text{ at } 90°)}{I_\gamma \text{ (at } 90° \text{ gated by } \gamma_G \text{ at } 35°/145°)}. \quad (1)$$

The DCO ratios for stretched electric quadrupole transitions are expected [1] to have values close to unity, while $\Delta I = 1$ transitions may have $R_{\rm DCO}$ values ranging from 0 to 2. However, $\Delta I = 1$ transitions with small $E2/M1$ mixing ratios δ are expected to have values of approximately 0.5.

Results of the level determinations, with energies, intensities, multipolarities, DCO ratios, and spin assignments are shown in Table I. Altogether 20 new transitions were identified, and another 6 were tentatively assigned, leading to 17 new excitation states and 2 tentative ones.

A. The positive-parity yrast band

The positive-parity yrast band of favored signature ($\alpha = +\frac{1}{2}$) was established in Ref. [7] to the $\frac{21}{2}^+$ level

TABLE I. Energies, intensities, and DCO ratios of γ decays in ^{77}Br.

E_x (keV)	I_i^π	I_f^π	E_γ (keV)	Intensity	$R_{\rm DCO}$	E_x (keV)	I_i^π	I_f^π	E_γ (keV)	Intensity	$R_{\rm DCO}$
129.5	$\frac{5}{2}^+$	$\frac{3}{2}^-$	129.5(1)	5	0.87(13)			$\frac{17}{2}^+$	1310.2(1)	18	0.70(7)
162.0	$\frac{5}{2}^-$	$\frac{3}{2}^-$	162.0(1)	60	0.67(3)	2932	$\frac{17}{2}^-$	$\frac{17}{2}^-$	592(1)	5	1.34(9)
417.1	$\frac{7}{2}^+$	$\frac{9}{2}^+$	311.5(3)	4	0.68(3)			$\frac{13}{2}^-$	1392(1)	5	0.99(10)
576.0	$\frac{7}{2}^-$	$\frac{5}{2}^-$	413.9(2)	5	0.43(6)	3037.2	$\frac{21}{2}^+$	$\frac{19}{2}^+$	(389)	<1	
		$\frac{3}{2}^-$	576.0(1)	18	0.92(6)			$\frac{17}{2}^+$	990.0(1)	18	1.16(7)
639.9	$\frac{13}{2}^+$	$\frac{9}{2}^+$	534.3(1)	100	1.01(4)	3201.2	$\frac{21}{2}^-$	$\frac{19}{2}^-$	408.4(6)	1	0.60(8)
782.7	$\frac{9}{2}^+$	$\frac{7}{2}^+$	365.1(8)	<1	0.79(7)			$\frac{17}{2}^-$	861.0(5)	35	1.00(6)
		$\frac{5}{2}^+$	653.2(6)	4	1.06(9)	3220	$(\frac{19}{2}^-)$	$\frac{17}{2}^-$	287.8(1)	4	0.89(1)
		$\frac{9}{2}^+$	676.8(3)	15	0.91(7)			$\frac{17}{2}^+$	1737(4)	2	0.85(5)
790.8	$\frac{9}{2}^-$	$\frac{7}{2}^-$	215.0(16)	3	0.94(28)	3610	$(\frac{21}{2}^-)$	$(\frac{19}{2}^-)$	390.3(1)	10	
		$\frac{5}{2}^-$	628.8(1)	51	1.00(3)			$\frac{21}{2}^+$	1059(1)	<1	
		$\frac{9}{2}^+$	685.1(3)	2	0.66(5)	3727.9	$\frac{23}{2}^+$	$\frac{19}{2}^+$	1080.1(1)	7	0.87(15)
947.1	$\frac{11}{2}^+$	$\frac{13}{2}^+$	307.4(1)	5	0.72(3)			$\frac{21}{2}^+$	(1177)	<1	
		$\frac{7}{2}^+$	530(1)	3		3729.9	$\frac{23}{2}^-$	$\frac{19}{2}^-$	936.6(4)	24	1.09(6)
		$\frac{9}{2}^+$	(842)	4		3775.5	$\frac{25}{2}^+$	$\frac{21}{2}^+$	1224.5(5)	34	1.06(7)
1274.8	$\frac{11}{2}^-$	$\frac{9}{2}^-$	483.5(9)	4	0.86(6)	4150	$(\frac{23}{2}^-)$	$(\frac{21}{2}^-)$	540(1)	7	
		$\frac{7}{2}^-$	698.8(2)	20	0.92(9)	4216.5	$\frac{25}{2}^+$	$\frac{21}{2}^+$	1179.3(4)	5	1.00(7)
1304.6	$\frac{13}{2}^+$	$\frac{11}{2}^+$	357(1)	2	0.84(7)	4247.5	$\frac{25}{2}^-$	$\frac{23}{2}^-$	(518)	<1	
		$\frac{9}{2}^+$	521.9(4)	13	1.06(5)			$\frac{21}{2}^-$	1046.3(3)	27	1.05(4)
		$\frac{13}{2}^+$	665.1(3)	13	0.94(6)	4903.1	$\frac{27}{2}^-$	$\frac{23}{2}^-$	1173.2(1)	8	1.03(7)
		$\frac{9}{2}^+$	1199.2(4)	10	0.92(7)	4980.7	$\frac{27}{2}^+$	$\frac{23}{2}^+$	1252.8(3)	7	1.00(9)
1482.5	$\frac{17}{2}^+$	$\frac{13}{2}^+$	842.6(2)	86	1.06(4)	5150.0	$\frac{29}{2}^+$	$\frac{25}{2}^+$	1374.5(5)	21	0.98(5)
1539.2	$\frac{13}{2}^-$	$\frac{11}{2}^-$	264.9(8)	2	0.71(6)	5517.6	$\frac{29}{2}^-$	$\frac{27}{2}^-$	(614)	<1	
		$\frac{9}{2}^-$	748.4(1)	43	0.97(4)			$\frac{25}{2}^-$	1270.1(3)	27	1.00(2)
		$\frac{13}{2}^+$	898(1)	2		5528.5	$\frac{29}{2}^+$	$\frac{25}{2}^+$	1312.0(5)	5	1.15(20)
1747.0	$\frac{15}{2}^+$	$\frac{17}{2}^+$	265(1)	<1	1.17(8)	6297	$\frac{31}{2}^-$	$\frac{27}{2}^-$	1394(1)	6	1.00(8)
		$\frac{11}{2}^+$	799.9(1)	15	0.98(9)	6410.4	$\frac{31}{2}^+$	$\frac{27}{2}^+$	1429.7(5)	<5	0.97(8)
		$\frac{13}{2}^+$	1108.6(5)	<1	0.68(1)	6692.1	$\frac{33}{2}^+$	$\frac{29}{2}^+$	1542.1(5)	16	1.10(8)
2022.2	$\frac{15}{2}^-$	$\frac{11}{2}^-$	747.4(1)	24	0.93(3)	6979.6	$\frac{33}{2}^-$	$\frac{29}{2}^-$	1462.0(4)	14	1.07(7)
		$\frac{13}{2}^+$	1381(1)	6	0.53(9)	7876	$(\frac{35}{2}^-)$	$\frac{31}{2}^-$	1579(1)	4	1.16(12)
2047.2	$\frac{17}{2}^+$	$\frac{15}{2}^+$	300(1)	<1	1.31(11)	8028	$\frac{35}{2}^+$	$\frac{31}{2}^+$	1618(1)	<5	1.11(13)
		$\frac{13}{2}^+$	742.6(5)	24	1.03(5)	8421	$\frac{37}{2}^+$	$\frac{33}{2}^+$	1729(3)	<5	0.96(10)
2340.2	$\frac{17}{2}^-$	$\frac{15}{2}^-$	317.8(2)	2	0.74(7)	8580	$(\frac{37}{2}^-)$	$\frac{33}{2}^-$	1600(1)	10	1.22(19)
		$\frac{13}{2}^-$	801.0(1)	38	1.03(6)	9609	$(\frac{39}{2}^-)$	$(\frac{35}{2}^-)$	1733(1)	2	
2551.0	$\frac{21}{2}^+$	$\frac{17}{2}^+$	1068.5(2)	55	1.07(3)	10281	$(\frac{41}{2}^-)$	$(\frac{37}{2}^-)$	1701(4)	<1	1.22(25)
2647.8	$\frac{19}{2}^+$	$\frac{15}{2}^+$	900.8(1)	7	1.04(5)	10316	$(\frac{41}{2}^+)$	$\frac{37}{2}^+$	1895(5)	<5	
		$\frac{17}{2}^+$	1165.2(5)	<1	0.66(8)	11344	$(\frac{43}{2}^-)$	$(\frac{39}{2}^-)$	(1735)	<1	
2793.3	$\frac{19}{2}^-$	$\frac{15}{2}^-$	771.1(1)	22	0.94(6)						

at 2548.4 keV and later extended [8] to $(\frac{25}{2}^+)$ at 3773.8 keV.

Transitions in coincidence with γ rays in this band are shown in Fig. 2. The lower-energy portion of the spectrum shown on top is the spectrum of γ rays in coincidence with the 534 keV $\frac{13}{2}^+ \rightarrow \frac{9}{2}^+$ transition, while the spectra in coincidence with the 534, 843, 1069, 1225, and 1375 keV transitions were added together to give better statistical accuracy for the higher-energy portion of the figure on the bottom. New transitions in the yrast sequence at 1375, 1542, and 1729 keV can be seen. These transitions have DCO ratios of essentially unity, consistent with stretched electric quadrupole transitions. An additional weak transition at 1895 keV is tentatively placed at the top of the decay scheme, but no DCO ratio could be measured for it.

The $\alpha = -\frac{1}{2}$ signature partner band was recently identified [8] up to the 2648 keV $(\frac{19}{2}^+)$ level. The present work has confirmed those states and extended the band up to the $\frac{35}{2}^+$ state at 8028 keV with four additional transitions. DCO ratios of about unity confirm stretched $E2$ character for all the transitions within this band.

B. Additional $\frac{9}{2}^+$ band

An additional positive-parity band was established [8] in ^{77}Br based on a second $\frac{9}{2}^+$ state at 783 keV. This band was extended from $(\frac{21}{2}^+)$ to $\frac{29}{2}^+$ in the present work. The DCO ratios of all the transitions within this band are consistent with stretched $E2$ decay. Although the $\frac{5}{2}^+$ state at 130 keV has the right spin to be a member of this band, neither its energy spacing nor the decay branching ratios support its inclusion within the band. The particle-rotor model calculations, discussed in Sec. IV B, suggest that this state is more closely related to the yrast band. Additional decays to the $\frac{7}{2}^+$ band were seen at 300 keV and tentatively at 389 keV. The decay strength in this excited band "bleeds" out near the bottom to all available positive-parity states.

C. The negative-parity bands

A pair of negative-parity bands built on the $\frac{3}{2}^-$ ground state was previously established [7] up to the 2338 keV $\frac{17}{2}^-$ state and recently extended [8] up to the 4246 keV

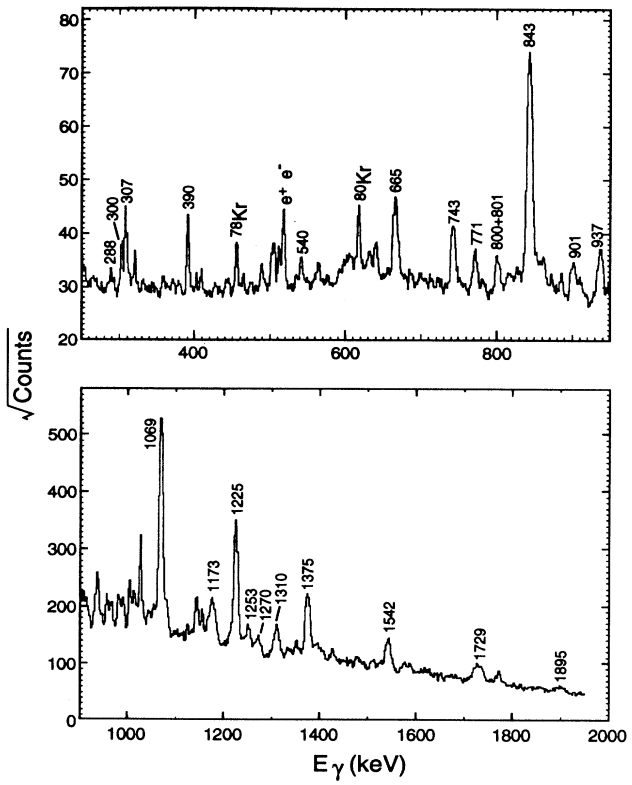

FIG. 2. The spectrum of γ rays in coincidence with the 534 keV $\frac{13}{2}^+ \rightarrow \frac{9}{2}^+$ transition (top) and in coincidence with the 534, 843, 1069, 1225, or 1375 keV transitions (bottom). Note that the square root of the number of counts is graphed on the ordinate to better show both strong and weak peaks.

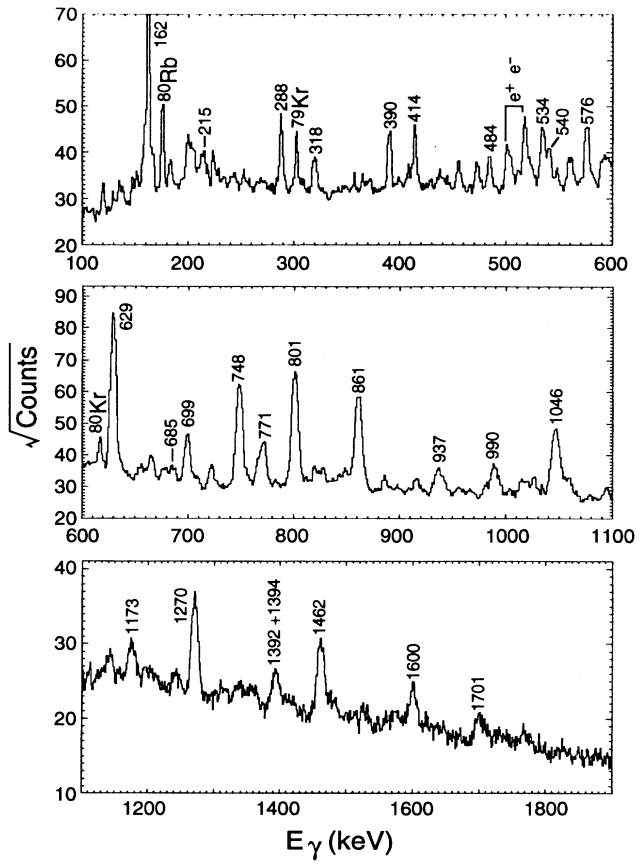

FIG. 3. The sum of γ spectra in coincidence with the 162, 748, and 1270 keV transitions.

$(\frac{25}{2}^-)$ state. The present work confirms these levels and extends them to $(\frac{41}{2}^-)$ at 10 281 keV and $(\frac{43}{2}^-)$ at 11 344 keV. The sum of spectra in coincidence with the 162, 748, and 1270 keV transitions is shown in Fig. 3. All the transitions within the $\alpha = +\frac{1}{2}$ band can be seen, along with some of those in the signature partner band and the $\Delta I = 1$ decays connecting the two bands. The DCO ratios of transitions in the favored band are in good agreement with the expected value of unity for stretched $E2$ decays through the 1462 keV transition. The larger error bars reflect poorer statistics for the unfavored sequence, but the DCO ratios are still consistent with stretched $E2$ decays through the 1394 keV transition.

Two γ rays near 1734 keV are in coincidence with each other, and the peak at this energy is approximately twice as strong as expected in gates placed on lower members of the unfavored signature band. This evidence suggests a close doublet. However, due to the limited statistical accuracy of these peaks, the upper transition of about 1735 keV has been indicated as tentative in the level scheme.

The second pair of negative-parity bands recently reported [8] based on the $(\frac{3}{2}^-)$ state at 167 keV was confirmed in the present experiment. It was not possible to observe any new states above the 1603 keV one in these bands due to their weak population and overlap with decays in other nuclei, such as the strong 616 keV transition in ^{80}Kr. Since no new information could be added, these bands are not shown in Fig. 1.

D. High-lying high-K band

An interesting decay sequence based on a $(\frac{17}{2}^-)$ state at 2932 keV was reported in Ref. [8]. Strong $\Delta I = 1$, but no $\Delta I = 2$ transitions, were observed. The sequence decays to both the positive- and negative-parity bands and appears analogous to other sequences which have been seen in ^{79,81}Br [9, 18], and ^{79,81,83}Rb [13, 19, 20]. The present work confirms this band. A new $(\frac{21}{2}^-) \rightarrow \frac{21}{2}^+$ decay branch was observed and a DCO ratio near unity for the 1392 keV transition provides a firmer spin assignment to the $\frac{17}{2}^-$ state.

The 288, 390, and 540 keV $\Delta I = 1$ transitions can be seen clearly in Figs. 2 and 3. The weak 288 keV line in the spectrum in coincidence with the 534 keV transition shown in Fig. 2 may result from the 1392 and 898 keV decay chain. We have not found any evidence for a direct decay from the $\frac{17}{2}^-$ state to the positive-parity band.

A three-quasiparticle (qp) configuration of $[\pi g_{9/2} \otimes \nu g_{9/2} \otimes \nu(p_{1/2}, p_{3/2}, f_{5/2})]$ was proposed for this band in Ref. [8]. Theoretical deformed shell-model calculations [21] also identify this configuration as the most likely. The fact that this 3qp configuration mixes very little with the low-lying negative-parity states in the calculations helps explain why the band does not decay preferentially to negative-parity states.

IV. DISCUSSION

A. Cranked-shell-model analysis

Since the knowledge of band structure in ^{77}Br has been extended to higher spins in the present work, it is instructive to perform a cranked-shell-model analysis to investigate band crossings, signature splitting, and the behavior of the moments of inertia. An inspection of the level schemes of the nearest odd-A isotopes, ^{75}Br [5, 6] and ^{79}Br [9], shows a considerable similarity to ^{77}Br. The cranking analysis has been extended to these nuclei as well. The moments of inertia of the positive-parity bands in ^{77}Br are compared with those of ^{75}Br and ^{79}Br in Fig. 4. The kinematic moments of inertia ($J^{(1)} = I_x/\omega$) are shown for all three positive-parity bands in ^{77}Br and the dynamic moments of inertia ($J^{(2)} = dI_x/d\omega$) are presented for the yrast favored signature ($\alpha = +\frac{1}{2}$) band.

The peak in the dynamic moment of inertia (bottom panel in Fig. 4) at $\hbar\omega \approx 0.6$ MeV for the yrast band in ^{75}Br has been interpreted [6] as a $\nu g_{9/2}$ alignment, since the lowest $\pi g_{9/2}$ crossing is Pauli blocked. The weaker

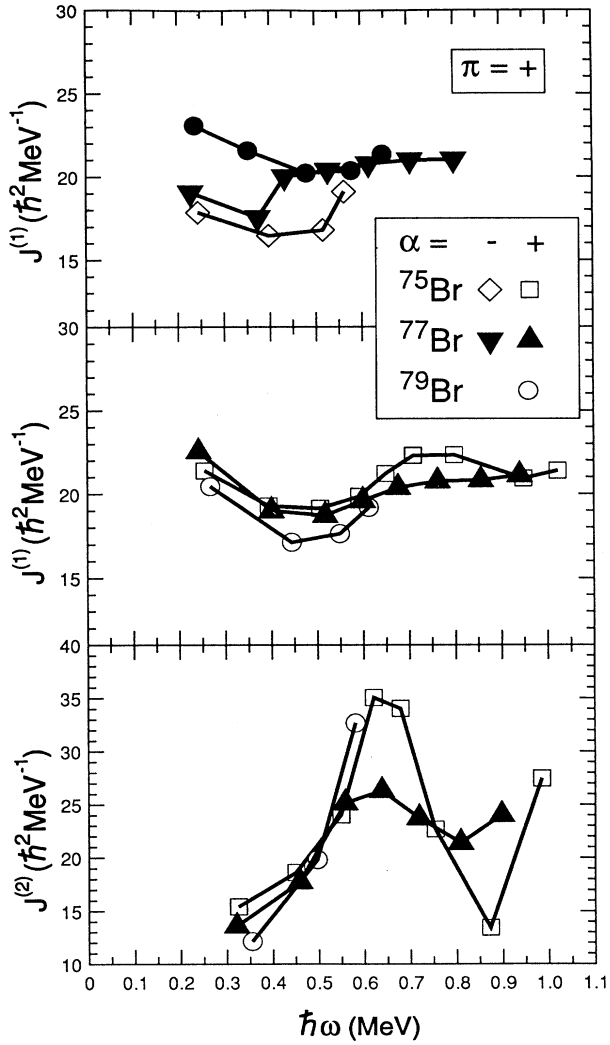

FIG. 4. Kinematic $J^{(1)}$ and dynamic $J^{(2)}$ moments of inertia as a function of rotational frequency ω for the positive-parity bands of ^{75}Br [5, 6], ^{77}Br, and ^{79}Br [9]. The sign of the signature quantum number α ($-\frac{1}{2}$ or $+\frac{1}{2}$) is indicated in the legend. $J^{(1)}$ values for the excited band based on the 783 keV $\frac{9}{2}^+$ state are shown with solid circles in the top graph.

peak for ^{77}Br probably corresponds to a similar alignment with a larger interaction. The ^{79}Br points suggest an alignment with at least as small an interaction as in ^{75}Br. It appears that the $\nu g_{9/2}$ alignment occurs at the same frequency but with different interaction strengths in all three isotopes, although the band is not known to high enough spins in ^{79}Br to confirm this picture. The highest frequency point for ^{75,77}Br may indicate the beginning of a second crossing.

In contrast, an upbend occurs at different frequencies in the kinematic moments of inertia of the unfavored ($\alpha = -\frac{1}{2}$) bands of ^{75,77}Br (top panel of Fig. 4). The moments of inertia of the third positive-parity band in ^{77}Br, also shown in the top panel of Fig. 4, become almost identical to those in the unfavored band for $\hbar\omega > 0.4$ MeV. In fact, all the kinematic moments of inertia appear to converge to about $21\hbar^2$/MeV, approximately the rigid-body value, in agreement with previously observed trends [22]. There are no known analogs in the neighboring Br isotopes for the excited $\frac{9}{2}^+$ band in ^{77}Br.

The experimental Routhians for most of the known bands in ^{75,77}Br are shown in Fig. 5. The reference rotor which has been subtracted is based on the Harris parameters, $J_0 = 15\hbar^2$/MeV and $J_1 = 3\hbar^4$/MeV^3. The positive-parity bands in both nuclei show very large signature splitting (up to 750 keV), indicative of rotation-aligned coupling. Such large signature splitting, seen as an inversion in the level ordering, also occurs in the Rb isotopes [14]. There is some decrease in the signature splitting in ^{77}Br at higher frequencies. In contrast, the signature splitting in ^{75}Br appears to be increasing up to the highest spin at which the unfavored signature band

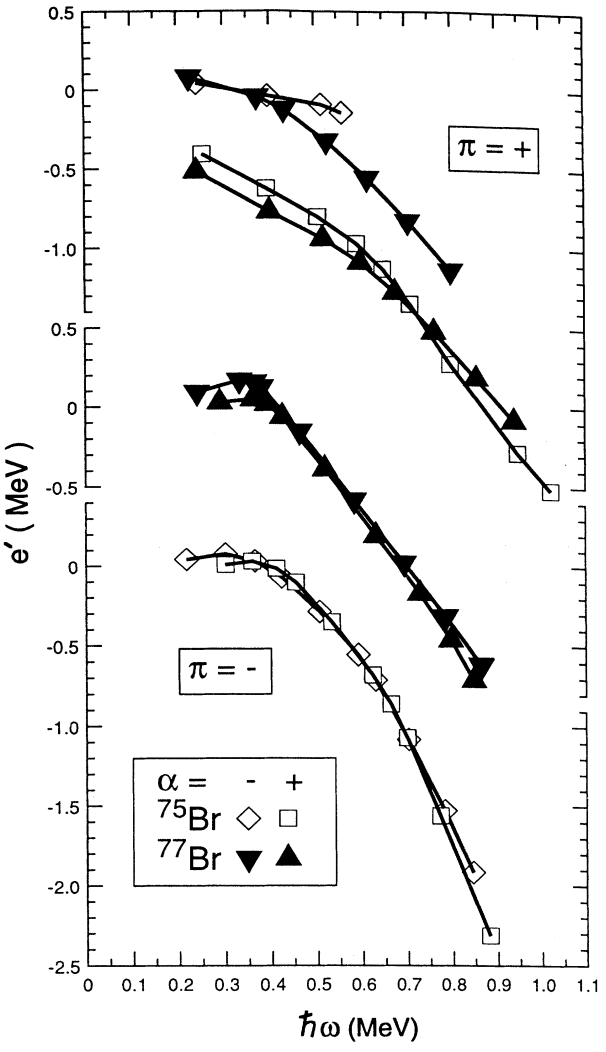

FIG. 5. Graphs of Routhians e' versus rotational frequency for the lowest positive- and negative-parity bands in ^{75}Br [5, 6] and ^{77}Br. Harris parameters of $J_0 = 15\hbar^2$/MeV and $J_1 = 3\hbar^4$/MeV^3 were used for the reference rotor. The sign of the signature α is indicated in the legend. Note that the Routhians for the negative-parity band of ^{75}Br are displaced relative to those for ^{77}Br for clarity, while those for the positive-parity bands are graphed on a common ordinate.

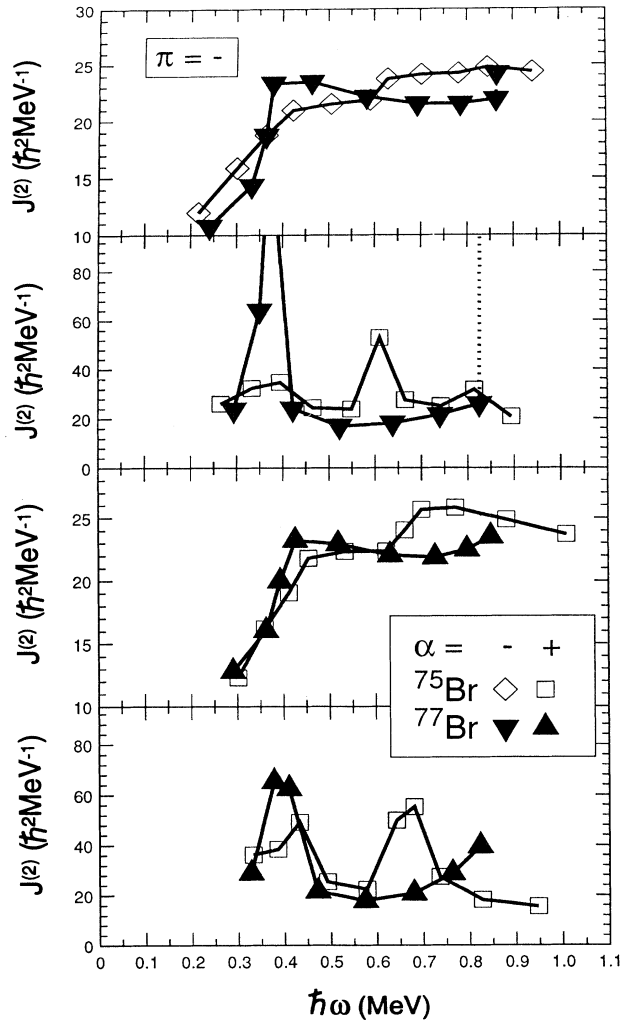

FIG. 6. Kinematic $J^{(1)}$ and dynamic $J^{(2)}$ moments of inertia as a function of rotational frequency ω for the negative-parity bands of ^{75}Br [5, 6] and ^{77}Br. The sign of the signature α is shown in the legend.

could be observed.

There is much less signature splitting in the negative-parity bands, as can be seen in Fig. 5. The largest is about 100 keV for the low-spin states in ^{77}Br. Although curves for ^{79}Br are not shown in Fig. 5 since it is not known to high spins, its Routhians indicate a somewhat larger signature splitting of about 200 keV at low spins. Thus, there appears to be a trend of increasing signature splitting with increasing mass for the low-spin states, which may be correlated with decreasing deformation as N increases toward the shell closure at $N = 50$.

The kinematic moments of inertia for the negative-parity bands of ^{75,77}Br, which are shown in Fig. 6, increase considerably at low spins and then appear to saturate at the rigid-body value. The last level in the $\alpha = -\frac{1}{2}$ band of ^{77}Br gives a sharp rise in $J^{(1)}$, but it should be treated as tentative with the present data. Two alignments can be seen in the $J^{(2)}$ graphs for ^{75}Br at rotational frequencies of about 0.4 and 0.65 MeV/$\hbar$. The first alignment has been interpreted [6] as a $\pi g_{9/2}$ crossing, which is Pauli blocked in the positive-parity band. The second has been interpreted as a $\nu g_{9/2}$ crossing, analogous to that seen in the positive-parity band. The lower frequency $\pi g_{9/2}$ alignment can also be seen in ^{77}Br, where it is even sharper. There is no sign of a second alignment in ^{77}Br below 0.7 MeV/$\hbar$. A gradual upbend appears to start at about 0.8 MeV/$\hbar$ in the $\alpha = +\frac{1}{2}$ band, while the sharp increase at 0.73 MeV/$\hbar$ in the $\alpha = -\frac{1}{2}$ band is only tentative. Thus, there is some evidence for the second alignment in ^{77}Br, but it is delayed relative to ^{75}Br and the interaction strength remains uncertain. This differs from the positive-parity bands, where the $\nu g_{9/2}$ crossing occurs at the same frequency in ^{75,77,79}Br.

B. Theoretical calculations

The Woods-Saxon cranking model of Nazarewicz *et al.* [23] was used to predict the shape of ^{77}Br. The rotation was treated by means of the cranking approximation with a monopole pairing force. More information about the calculation is given in Refs. [1, 24].

Typical total Routhian surfaces (TRS) from the calculation are shown in Fig. 7. Those shown for a rotational frequency of $\hbar\omega = 0.3$ MeV are typical of the surfaces below the first band crossing, while those for 0.7 MeV give an indication of the shape changes predicted after the alignments. The graphs for the unfavored signature $\alpha = -\frac{1}{2}$ are generally similar to those shown for $\alpha = +\frac{1}{2}$. Considerable γ softness is predicted in the 1qp bands of both positive "A" and negative "F" parity. A moderately strong deformation of $\beta_2 \approx 0.3$ is predicted, in agreement with the measured [15] $B(E2)$ values.

After the alignments at $\hbar\omega = 0.7$ MeV the nucleus is predicted to become more γ stiff, and a triaxial shape with $\gamma \approx -30°$ is predicted for both parities. This shape change may give rise to the reduction in signature splitting seen in Fig. 5.

Calculations of the energy level scheme were made using the triaxial particle-rotor model [25,26] with standard parameters [27] for the modified harmonic oscillator po-

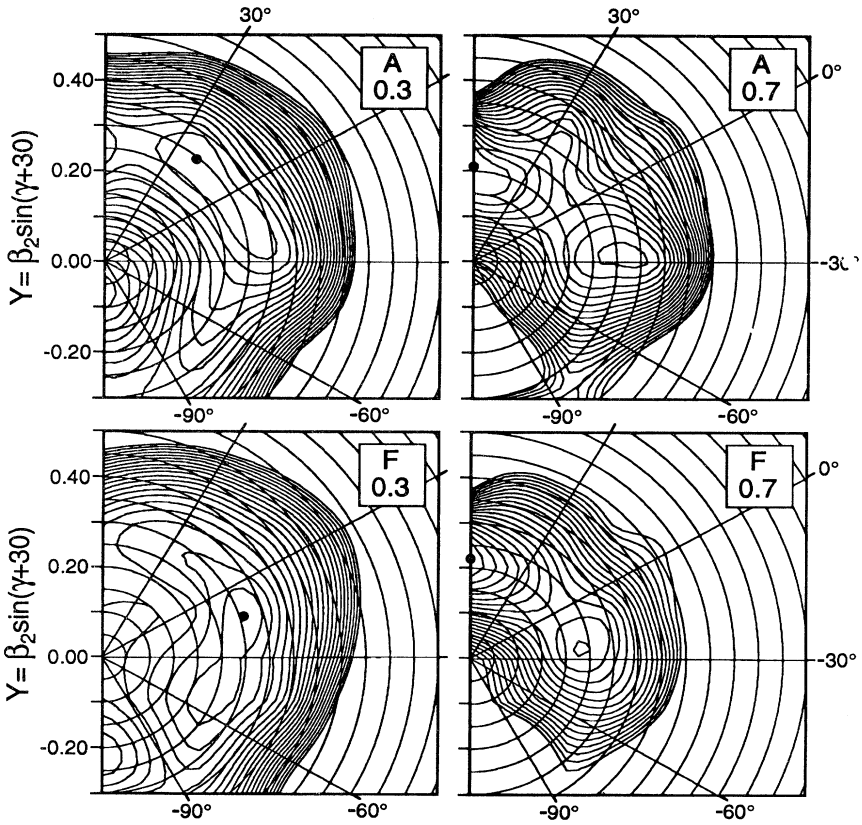

FIG. 7. Theoretical total Routhian surfaces for ^{77}Br as a function of the quadrupole deformation parameters β_2 and γ. The upper graphs are for the lowest $\pi = +$, $\alpha = +\frac{1}{2}$ configuration "A," while the lower ones represent the lowest $\pi = -$, $\alpha = +\frac{1}{2}$ configuration "F." The left (right) graphs are calculated for a rotational frequency $\hbar\omega = 0.3$ MeV (0.7 MeV).

tential. A variable moment of inertia was used for the rotor based on Harris parameters of $J_0 = 14.7\hbar^2/\text{MeV}$ and $J_1 = 10.2\hbar^4/\text{MeV}^3$ fitted to the yrast band of ^{78}Kr. A Coriolis attenuation factor of $\xi = 0.7$ was used. The nuclear shapes were taken from those predicted by the Hartree-Fock-Bogolyubov cranking calculations of Fig. 7. For the positive-parity band the minimum in the collective sector was used. The corresponding modified oscillator shape parameters are $\epsilon_2 = 0.29$, $\gamma = 15°$, and $\epsilon_4 = 0.045$. Note that the collective sector in the cranking model, $\gamma = 0°$ to $-60°$, corresponds to the region $\gamma = 0°$ to $+60°$ in the particle-rotor model. In the negative-parity band at low frequencies the nearly prolate and nearly oblate minima have roughly equal energies. Calculations were made for both of these shapes. The parameters are $\epsilon_2 = 0.28$, $\gamma = 13°$, and $\epsilon_4 = 0.03$ for the near prolate minimum and $\epsilon_2 = 0.22$, $\gamma = 56°$, and $\epsilon_4 = 0.03$ for the near oblate shape.

The results of the particle-rotor model (RPC) calculations are shown in Fig. 8 along with the experimental levels. The RPC results for the positive-parity bands correctly reproduce the large signature splitting and level inversion. However, they do not predict the slight reduction in signature splitting, which occurs above the $\frac{21}{2}^+$ state. This may well be due to a change in triaxiality in this γ-soft nucleus. At higher spins the predicted level energies are somewhat lower than experiment. This phenomenon has often been seen in RPC calculations for bands based on unique-parity orbitals such as $g_{9/2}$. Such a level depression was recently seen in calculations [13] for ^{79}Rb. Calculations along somewhat similar lines have also been made in the past [7, 15]. These calculations also tended to overpredict the degree of signature splitting. For example, the $\frac{7}{2}^+$- $\frac{13}{2}^+$ level ordering is inverted in those calculations as well as the present one. Those of Ref. [15] used a similar deformation of $\beta_2 = 0.3$, although it is not clear what degree of triaxiality was used.

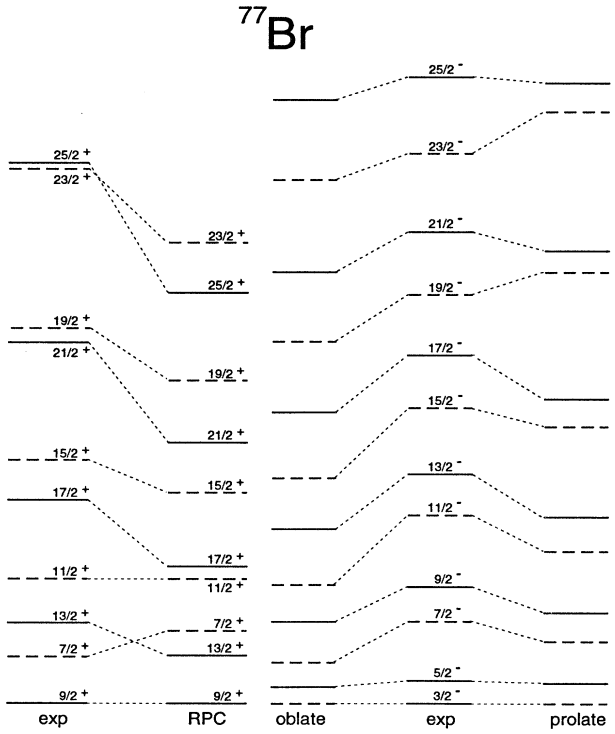

FIG. 8. A comparison of the experimental level scheme of ^{77}Br with particle-rotor model calculations discussed in the text. States with unfavored signature ($\alpha = -\frac{1}{2}$) are drawn with dashed lines to make the comparison of level ordering clearer.

A $\frac{5}{2}^+$ state, which may correspond to the one observed at 130 keV, is also predicted in the present RPC calculations within 3 keV of the $\frac{9}{2}^+$ level. The large calculated $B(E2)$ strength between these two states of 75 Weisskopf units (W.u.) is comparable to that between other members of the yrast band and suggests that the 130 keV state is a member of the yrast band, rather than the excited band which includes the 783 keV state. In addition, the measured lifetimes [15] of the 783 and 1305 keV states imply $B(E2)$ strengths of 21 W.u. for the 653 keV transition and 78 W.u. for the 522 keV decay. While the latter value is typical of intraband transitions in ^{77}Br, the lower strength of the 653 keV decay suggests more of the character of an interband transition. Therefore, it appears that the wave function of the 130 keV state overlaps more with the yrast band than the excited band. It is shown displaced from the yrast band in Fig. 1 only for clarity.

Another band with strong intraband $E2$ decays is predicted by the RPC calculations. This may correspond to the observed band based on the 783 keV level, although the predicted energies are about 350 keV too high.

A significant amount of signature splitting is predicted for the negative-parity bands if the nuclear shape is nearly prolate. By contrast, there is very little signature splitting predicted for the nearly oblate shape. The experimental values are intermediate. The moderate signature splitting observed at low spins is similar to that predicted for the prolate shape, while the absence of signature splitting at higher spins resembles the RPC results for oblate shape. It is possible that the shape of the negative-parity structure shifts from nearly prolate to nearly oblate with increasing spin. This would be consistent with the TRS calculations in Fig. 7 which show that the two shapes are almost equally favored energetically.

For comparison, we note that similar TRS calculations for the isotone ^{79}Rb [13] predict well-defined triaxiality with no γ softness. In this case the RPC calculations agree better with experiment, and the observed signature splitting remains more constant. This would support the interpretation that the variable signature splitting and poorer agreement with RPC calculations in ^{77}Br result from γ softness leading to shape variability.

V. SUMMARY

The high-spin structure of ^{77}Br was investigated using the ^{65}Cu(^{18}O,$\alpha 2n$)^{77}Br reaction at 65 MeV and the Pitt-FSU γ-detection array. The level scheme of Ref. [8] was verified and 19 new states and 26 new transitions were added. Firm spin assignments were established up to

spins of $\frac{33}{2}^-$ and $\frac{37}{2}^+$ using the measured DCO ratios.

A presumed $\nu g_{9/2}$ alignment is seen in the positive-parity band at the same rotational frequency ($\hbar\omega \approx 0.6$ MeV) as in ^{75,79}Br, although the interaction strength is larger. In the negative-parity band the lowest $\pi g_{9/2}$ crossing occurs at the same frequency as in ^{75}Br, but the upper $\nu g_{9/2}$ crossing is delayed and evidence for the beginning of this alignment is only tentative. The very large signature splitting ($\approx$750 keV) in the positive-parity bands decreases at higher spins. Although the signature splitting in the negative-parity bands is much less ($\approx$100 keV), it is larger than in ^{75}Br and decreases at higher spins.

The total Routhian surfaces calculated in the Woods-Saxon cranking model predict considerable γ softness or the coexistence of shapes with different γ parameters. Particle-rotor model calculations based on the predicted triaxial shape for the positive-parity configuration reproduce the inverted level ordering resulting from the large signature splitting but do not reproduce the decreasing signature splitting seen at higher spins. For the negative-parity bands, RPC calculations based on the predicted nearly prolate shape correctly reproduce the moderate signature splitting at low spins, while those based on the nearly oblate shape reproduce the absence of signature splitting at higher spins. These results suggest that the change in signature splitting in both bands may reflect changes in triaxiality with spin in both bands, in confirmation of the predicted γ softness.

ACKNOWLEDGMENTS

We wish to thank W. Nazarewicz for providing the Woods-Saxon cranking model results and P. Semmes and I. Ragnarsson for providing the particle-rotor codes used. We are grateful to J.X. Saladin, whose loan of the University of Pittsburgh detectors made the combined array possible. This work was supported in part by the National Science Foundation. The initial research of G.N.S. was supported by an NSF Research Experience for Undergraduates Fellowship Program.

[1] E.F. Moore, P.D. Cottle, C.J. Gross, D.M. Headly, U.J. Hüttmeier, S.L. Tabor, and W. Nazarewicz, Phys. Rev. C **38**, 696 (1988).

[2] T.D. Johnson, T. Glasmacher, J.W. Holcomb, P.C. Womble, S.L. Tabor, and W. Nazarewicz, Phys. Rev. C **46**, 516 (1992).

[3] J. Heese, K.P. Lieb, L. Lühmann, S. Ulbig, B. Wörmann, D. Alber, H. Grawe, H. Haas, and B. Spellmeyer, Phys. Rev. C **36**, 2409 (1987).

[4] J. Heese, N. Martin, C.J. Gross, W. Fieber, K.P. Lieb, A. Kuhnert, K.H. Maier, and X. Sun, Phys. Rev. C **41**, 1553 (1990).

[5] N. Martin, C.J. Gross, J. Heese, and K.P. Lieb, J. Phys. G **15**, L123 (1989).

[6] L. Lühmann, M. Debray, K.P. Lieb, W. Nazarewicz, B. Wörmann, J. Eberth, and T. Heck, Phys. Rev. C **31**, 828 (1985).

[7] M.A. Deleplanque, C. Gerschel, N. Perrin, and B. Ader, J. Phys. (Paris) **35**, L237 (1974).

[8] J. Döring, L. Funke, R. Schwengner, and G. Winter, this issue, Phys. Rev. C **48**, xxxx (1993); in *Nuclear Structure in the Nineties*, edited by N. Johnson (Oak Ridge National Laboratory, Oak Ridge, Tennessee, 1990), p. 84.

[9] R. Schwengner, J. Döring, L. Funke, H. Rotter, G. Winter, A. Johnson, and A. Nilsson, Nucl. Phys. **A486**, 43 (1988).

[10] K.P. Lieb, L. Lühmann, and B. Wörmann, in *Nuclei Off the Line of Stability*, ACS Symposium Series No. 324, edited by Richard A. Meyer and Daeg S. Brenner (American Chemical Society, New York, 1986).

[11] L. Lühmann, K.P. Lieb, C.J. Lister, B.J. Varley, J.W. Olness, and H.G. Price, Europhys. Lett. **1**, 623 (1986).

[12] Ö. Skeppstedt, C.J. Lister, A.A. Chishti, B.J. Varley, W. Gelletly, U. Lenz, R. Moscrop, and L. Goettig, Nucl. Phys. **A511**, 137 (1990).

[13] J.W. Holcomb, J. Döring, T. Glasmacher, G.D. Johns, T.D. Johnson, M.A. Riley, P.C. Womble, and S.L. Tabor, Phys. Rev. C **48**, 1020 (1993).

[14] S.L. Tabor, P.D. Cottle, C.J. Gross, U.J. Hüttmeier, E.F. Moore, and W. Nazarewicz, Phys. Rev. C **39**, 1359 (1989).

[15] H. Schäfer, A. Dewald, A. Gelberg, U. Kaup, K.O. Zell, and P. von Brentano, Z. Phys. A **293**, 85 (1979).

[16] S.L. Tabor, M.A. Riley, J. Döring, P.D. Cottle, R. Books, T. Glasmacher, J.W. Holcomb, J. Hutchins, G.D. Johns, T. Petters, O. Tekyi-Mensah, P.C. Womble, L. Wright, and J.X. Saladin, Nucl. Instrum. Methods B **79**, 821 (1993).

[17] S.L. Tabor, Nucl. Instrum. Methods A **265**, 495 (1988).

[18] L. Funke, J. Döring, P. Kemnitz, P. Ojeda, R. Schwengner, E. Will, G. Winter, A. Johnson, L. Hildingsson, and Th. Lindblad, Z. Phys. A **324**, 127 (1986).

[19] W. Wagner, L. Funke, J. Döring, L. Käubler, R. Schwengner, and G. Winter, Rossendorf Annual Report No. ZFK-667, 28 (1989).

[20] W. Gast, K. Dey, A. Gelberg, U. Kaup, F. Paar, R. Richter, K.O. Zell, and P. von Brentano, Phys. Rev. C **22**, 469 (1980).

[21] R. Sahu and S.P. Pandya, Nucl. Phys. **A529**, 20 (1991).

[22] S.L. Tabor, Phys. Rev. C **45**, 242 (1992).

[23] W. Nazarewicz, J. Dudek, R. Bengtsson, T. Bengtsson, and I. Ragnarsson, Nucl. Phys. **A435**, 397 (1985).

[24] U.J. Hüttmeier, C.J. Gross, D.M. Headly, E.F. Moore, S.L. Tabor, T.M. Cormier, P.M. Swertka, and W. Nazarewicz, Phys. Rev. C **37**, 118 (1988).

[25] S.E. Larsson, G. Leander, and I. Ragnarsson, Nucl. Phys. **A307**, 189 (1978).

[26] Paul B. Semmes and Ingemar Ragnarsson, in *High Spin Physics and Gamma-Soft Nuclei*, edited by J.X. Saladin, R.A. Sorensen, and C.M. Vincent (World Scientific, Singapore, 1990), p. 500.

[27] T. Bengtsson and I. Ragnarsson, Nucl. Phys. **A436**, 14 (1985).